High-Speed Wireless Indoor Communication via Visible Light

J. Grubor[1], O.C. Gaete Jamett[2], J.W. Walewski[2], S. Randel[2], K.-D. Langer[1]
[1]Fraunhofer Institute for Telecommunications, Heinrich-Hertz-Institut, Einsteinufer 37, 10587 Berlin
[2]Siemens Corporate Technology, Information and Communications, Networks and Multimedia Communications, Otto-Hahn-Ring 6, 81730 Munich
e-mail: grubor@hhi.fraunhofer.de

Zusammenfassung: *Durch doppelte Nutzung ermöglichen Weißlicht-LEDs Synergie von Raumbeleuchtung und drahtloser optischer Kommunikation/ Nachrichtenverteilung. Für einen mit LEDs gut ausgeleuchteten mittelgroßen Büroraum wird die erreichbare Datenrate bei Basisband- und DMT-Übertragung ermittelt, wobei der Einsatz handelsüblicher LEDs und Photodioden angenommen wird. Die Resultate zeigen, dass trotz relativ geringer Systembandbreite Bitraten von mehr als 100 Mbit/s zu erwarten sind.*

Summary: *Emergence of white-light LEDs allows synergy of lighting and broadcast/communication function in one optical source. We investigate possible data transmission rates in a moderate-size office room where we assume illumination conforming to standards and the use of commercially available LEDs and photodiodes. The performances of systems relying on base-band and DMT transmission show that data rates of more than 100 Mbit/s can be expected despite the rather low bandwidth of the system.*

1. Introduction

Optical wireless technology presents a promising supplement to its counterpart, which is based on radio (RF) transmission (e.g., WLAN). It offers huge, worldwide available and free bandwidth without EMI with radio bands, which makes it very attractive for RF-sensitive operating environments. Especially in case of visible light, there exists a noticeable synergetic potential for simultaneous use of light sources for lighting and communication.

The idea of bringing these two worlds together was recently re-invigorated through the emergence of white-light LEDs, which offer a considerable modulation bandwidth (~20 MHz). Moreover, such LEDs posses clear advantages over conventional lighting sources, which make them a strong candidate for future illumination scenarios. With visible-light wireless systems it would be possible to broadcast various broadband information in offices, or public transport, as well as to use internet or a mobile phone, even on board of aircrafts. Going even further, one could imagine communication between cars or to street hubs, or between machines (robots).

Optical wireless communication systems utilizing white LEDs were recently proposed in the literature, [1-6]. Several of these investigations relied on complex tri-chromatic LEDs with idealized bandwidths of 100 MHz and more, [1-3]. Also, the use of narrow-band Discrete Multitone (DMT) signals was considered in [4, 5]. In [6], the focus was on low-bit-rate transmission for automobile communication. In our study we revisit the work of Komine *et. al.*, [2], but consider realistic and commercially available "single chip" LEDs (blue LED plus phosphor). By theoretical analysis we investigate the potentials for high-speed transmission in a moderate-size office, both with base-band and DMT modulation.

This paper is organized as follows. Section 2 discusses the lighting characteristics of state-of-the-art LED chips and, starting from the standard requirements for brightness at the desk-top surface, two design scenarios are chosen for more detailed investigations. In Section 3, potential transmission rates are investigated for these scenarios. The transmission channel is defined, inter-symbol interference is discussed, and achievable data rates with base-band and DMT transmission are derived. Furthermore, the complexity of the regarded systems is briefly discussed. Section 4 provides summary and conclusions.

2. Illumination via White LEDs

2.1 Framework for Investigation

In order to be able to compare our results with those from [2], we consider the same model room, given in **Fig. 1** (5x5x3 m^3, with optical sources installed 2.5 m from the floor). Because of the assumed office or home environment, we evaluate the system performance at the desk-top height (0.85 cm from the floor).

For proper lighting a certain brightness of the illuminated surface is required, and, for reliable transmission sufficient optical power is needed. Both of these conditions need to be included in system design.

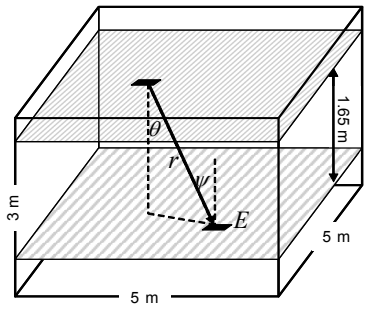


Figure 1: Model room. Definition of the shown parameters is given in Section 2.2

2.2 LED Chip Characteristics

Even though white light can be produced by proper mixing of red, green and blue light (3 chips), most of the present white LEDs are based on a blue LED chip topped with a YAG phosphor layer. The power spectrum of such an LED, [7], which was measured in our laboratory, is shown in **Fig. 2**.

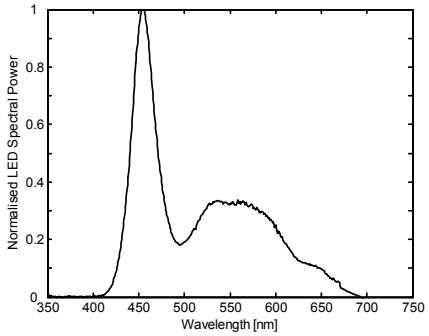


Figure 2: Measured radiation spectrum of LED [7]

From its radiation spectrum, one can obtain the luminous flux, Φ [lm], of the source as

$$\Phi = 683\frac{\text{lm}}{\text{W}}\int_{380\,\text{nm}}^{720\,\text{nm}} p(\lambda)V(\lambda)d\lambda\,, \qquad (1)$$

where $p(\lambda)$ [W/m] and $V(\lambda)$ denote the source power spectral distribution and the eye sensitivity function [8], respectively. The luminous flux presents optical power of the source as perceived by the human eye. The parameter of interest for us is the illuminance, E [lx], which expresses the brightness of the illuminated surface. It is defined as luminous flux per unit area

$$E \triangleq \partial\Phi/\partial A = I(\theta)/r^2\,, \qquad (2)$$

and depends on the source luminous intensity, $I(\theta)$ [cd], in the direction θ, reflecting the radiation pattern, and the distance to the illuminated surface, r (see **Fig. 1**). When a source with Lambert radiation characteristic is assumed and the angle of incidence ψ, is accounted for, the horizontal illuminance is

$$E_h = I_0\cos^m(\theta)\cos\psi/r^2 \qquad (3)$$

where $I_0 = I(\theta=0) = (m+1)\Phi/(2\pi)$ is the maximal luminous intensity. The Lambert index, m, defines the source radiation semi-angle as $m = -1/\log_2(\cos\theta_{\max})$.

Relevant parameters for data transmission are optical source power and modulation bandwidth. **Figure 3** shows the measured modulation bandwidth of LED [7]. One can see that, by suppressing the slow phosphorescent portion of the optical spectrum (~500-700 nm), modulation bandwidth can be enhanced to ~20 MHz.

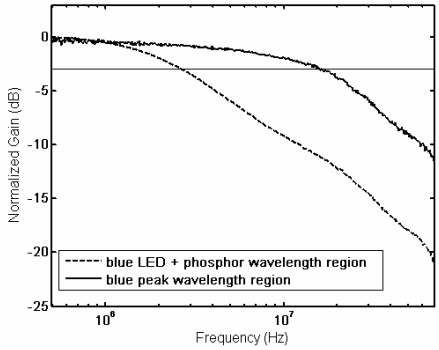


Figure 3: Measured modulation bandwidth of LED [7]

The source optical power, P [W] (radiant flux) has no relationship to the eye sensitivity and is given as

$$P = \int p(\lambda)d\lambda\,. \qquad (4)$$

By measuring $p(\lambda)$ and knowing $V(\lambda)$, both P and Φ were evaluated and a conversion factor of 4.2 lm/mW for this type of LEDs was obtained. Estimation was that the blue peak contains about 50% of the source power, leading finally to the expression for optical power available in the blue peak region (for a source with luminous flux Φ)

$$P_T[\text{mW}] = \alpha[\text{mW/lm}]\Phi[\text{lm}] = 2.1\Phi\,. \qquad (5)$$

Although bandwidth measurement and conversion-factor calculation were done for a particular LED [7], it is reasonable to use the obtained values for other chips manufactured in a similar way.

2.3 Fulfilling the Lighting Function

We first intend to secure enough horizontal brightness at the desk-top surface. We regard 400 lx as a minimal recommendable brightness at the desk-top height in the area where a working place is set, and aim for a 200-800 lx span in the whole room (in accordance with DIN5035, [9]).

Throughout our study, we investigated several commercially available LEDs and concluded that using a chip with large radiation angle is of practical importance, since in this case only a moderate number of chips suffice for room illumination. We assume one LED chip [10], whose characteristics are given in **Table 1**. The figures for radiation angle and possible luminous intensity were provided by the manufacturer, and the output optical power by Eq. (5).

Table 1. Relevant parameters and statistics

Parameter	**Scenario A**	**Scenario B**
LED characteristics		
$2\theta(m)$	120° (1)	
I_0	9.5 cd	
P_T	63 mW	
Scenario characteristics		
LED distribution across the ceiling	uniform	4 lamps
LED chip spacing	16 cm	7 cm
Number of chips	961	784
Brightness statistics		
E (min, max)	(237,855) lx	(181,855) lx
$E \geq 400$ lx	89.7 %	80.2 %
Transmission statistics		
max LOS delay	5.5 ns	
Channel min f_{3dB}	>200 MHz	98 MHz
P_R (min, av, max)	(0.1, 0.4, 0.5) mW	
SNR (min, max)	(49, 60) dB	(47, 60) dB
$SNR \geq 54.5$ dB	88%	79%

Two scenarios were considered suitable for further investigation, both of them using the same LED chip. Scenario A considers a ceiling that is uniformly covered with 16-cm-spaced LEDs, whereas, in scenario B, four distinct surfaces (referred to as lamps), contain 7-cm-spaced LEDs. It is assumed that one LED chip covers a surface of 1 cm^2. Both scenarios foresee less than 1000 chips (**Table 1**). As a comparison, in [2] over 14000 chips were considered in the same room model. In **Fig. 4**, the ceiling design for the two scenarios is given, and **Fig. 5** shows the corresponding distributions of E at the desk-top surface. Due to the symmetry of configurations, only a portion of the desk-top surface (directly under the areas within dashed lines in **Fig. 4**) is presented in **Fig. 5**.

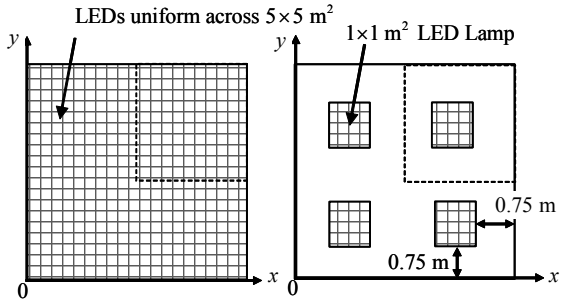


Figure 4 : Ceiling scenario design (left: A, right: B).

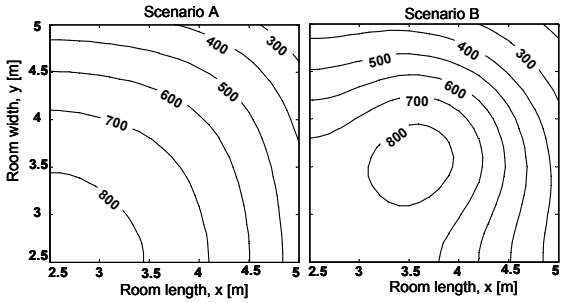


Figure 5: Horizontal brightness distribution, E[lx] at the desk-top surface, under the dashed areas of Fig.4

From **Fig. 5** can be seen that, in both scenarios, the aimed brightness span was obtained, with a major portion of the surface getting at least 400 lx, thus being suitable for a work place. The exact statistics are given in **Table 1**.

3. Data Transmission via White LEDs

3.1 Communication Channel

The channel to one point at the receiving surface, includes a number of lines-of-sight, LOS (stemming from different LED chips) as well as a contribution of reflections off the walls or objects in the room. The LOS contributions can be modelled by Dirac pulses, whereas the diffuse portion can be represented by an exponential function as in [11] (integrating sphere model). The channel frequency response can then be written as

$$H(f) = \sum_i \eta_{LOS,i} \exp\left(-j2\pi f \Delta\tau_{LOS,i}\right) + \eta_{DIFF} \frac{\exp\left(-j2\pi f \Delta\tau_{DIFF}\right)}{1 + j f / f_0}, \quad (6)$$

where η_{LOS} and η_{DIFF} present the channel gain for the LOS and diffuse signal respectively, $\Delta\tau$ the corresponding signal delays, and f_0 the cut-off

frequency of the purely diffuse channel. Hereby, the LOS gain from the i^{th} LED chip is

$$\eta_{LOS,i} = A_R (m+1)\cos^m \Phi_i \cos\psi_i / (2\pi r_i^2), \quad (7)$$

where A_R is the effective receiver surface (together with filter and concentrator gain). We assume a commercially available photodiode with 1 cm^2 surface [12], and follow [2] by choosing a concentrator gain of 3 (120° FOV), together with an ideal filter, summing up to an effective surface of $A_R = 3$ cm^2. According to the assumed model, the diffuse signal gain is constant everywhere in the room, and depends on A_R and room properties (size, A_{ROOM} , and average reflectivity, ρ)

$$\eta_{DIFF} = A_R \rho / A_{ROOM} (1-\rho). \quad (8)$$

The cut-off frequency, f_0 depends on the room properties, and is about 10 MHz for a medium-sized room, [11]. Nevertheless, as it will be shown below, this will have no significant influence.

3.2 ISI Discussion

Inter-symbol interference occurs due to multipath propagation, and limits the transmission speed in non-directed systems. The amount of ISI will depend on the chosen transmission scenario (room properties, distribution of chips at the ceiling and chip properties itself). We assume that all signal replicas, arriving at the receiver with more than half of the symbol period delay (after the first signal), contribute to ISI. Therefore,

$$P_{R,sig} = \sum_i P_R (t_i \le T_s/2) \text{ and } P_{R,ISI} = \sum_i P_R (t_i > T_s/2), \quad (9)$$

for the received optical signal power. Given that the transmitted signal is limited to 20 MHz (LED modulation bandwidth), the symbol period is limited to 50 ns, and ISI will occur if some replicas have delays larger than 25 ns.

We investigated the presence of ISI in the considered room for both scenarios. First, the maximal delay between two LOS optical paths was determined by the maximal radiation angle of the used source, and the distance between transmitter and the desk-top surface. In our case, this delay is 5.5 ns, so the ISI stemming from different LOS paths is not present. Second, to determine the influence of signals coming via diffuse reflections, we have obtained the cut-off frequency of the total channel all the over desk-top surface, according to

$$|H(f_{3dB})|^2 = 0.5|H(0)|^2. \quad (10)$$

The minimal cut-off frequencies (worst location at the desk-top surface) for scenarios A and B are given in Table 1. In both cases $f_{3dB} \gg 20$ MHz . Therefore, the channel is flat over the considered bandwidth, and the influence of ISI can be neglected. All LOS signal components arrive at the receiver within less than half of the symbol time and the influence of diffuse reflections is suppressed by strong LOS light all over the room. Nevertheless, even with T_s=50 ns, ISI can be encountered in large rooms with high ceilings (e.g., conference halls).

3.3 Received Optical Power and Obtained SNR

In the flat channel, received optical signal power is the sum of the powers coming from all chips

$$P_R = \sum_i |H_i(0)| P_{T,i} = \sum_i \eta_{LOS,i} P_{T,i}. \quad (11)$$

The *SNR* is then given by

$$SNR = \gamma^2 P_R^2 / (N_0 B), \quad (12)$$

where γ [A/W] denotes receiver responsivity, and N_0 the noise power spectral density [A^2/Hz] over the bandwidth B (20 MHz). The responsivity of Si-based photodiodes is ~0.28 A/W in the blue region. The dominant noise factor is the shot-noise increase stemming from received ambient light. Bright sky induces a photocurrent of I_{al} = 27 mA at the receiver, and the noise order of magnitude is

$$N_0 \cong N_{shot} = 2qI_{al} \sim 10^{-21} \text{ A}^2/\text{Hz}, \quad (13)$$

where q is the electron charge.

Figure 6 presents the *SNR* distributions at the desk-top surface. Exact spans of the received power and *SNR* are given in **Table 1**. Since the *SNR* is not affected by ISI, it remains above 47 dB over the whole surface. After simple mathematical transformations, the *SNR* can be expressed over the brightness level, E

$$SNR = E^2 (\gamma A_R \alpha)^2 / (N_0 B). \quad (14)$$

For 400 lx, *SNR* is a little above 54.5 dB, making this the minimal *SNR* in the recommended working surface (covering ~90% and ~80% of the desk-top surface for scenarios A and B, respectively).

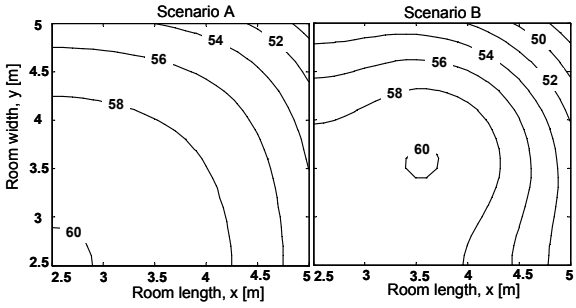


Figure 6: *SNR* [dB] distribution

3.4 Achievable Transmission Speed

In our system, the signal bandwidth is limited to 20 MHz by the modulation bandwidth of the LED. If raised-cosine pulses with β=1 roll-off factor are assumed, bit rates higher than 20 Mb/s can be achieved if bandwidth efficient modulation formats (MF) are used. Due to IM/DD type of optical wireless systems, *M*-PAM is the only bandwidth-efficient MF for base-band transmission. It is, however, known that *M*-QAM has better power efficiency than *M*-PAM (also better than *M*-PSK), but this type of modulation is only possible in our system if subcarrier modulation is used. In the following, we evaluate and compare performances of a base-band transmission (using *M*-PAM), and a subcarrier-based system, relying on DMT with *M*-QAM modulation. We will primarily consider the already introduced scenarios (no ISI), but will also discuss the performances if ISI occurs.

In general, subcarrier modulation enhances system robustness in an ISI-susceptible environment. In an optical wireless system, it also offers better robustness against ambient-light noise, which is particularly strong around dc.

In particular, DMT is a special type of modulation/multiplexing technique, that offers very high bandwidth efficiency, deals with ISI inherently, allows for the simplest equalization at the receiver, and can be entirely realized by digital signal processing, [13]. In DMT, information is mapped with *M*-QAM, and separated to *K* QAM-symbol streams, which are multiplexed by an IFFT block to realize a modulating signal at the transmitter. At the receiver, the process is vice-versa. DMT realizes a real-valued output from IFFT, by performing a conjugate-symmetry of its input signal. This operation enforces doubling the number of IFFT ports and of the DAC bandwidth However, for a small number of subcarriers which is considered here, this is quite irrelevant.

The total transmission rate *R* [bit/s] in the *M*-PAM base-band system is

$$R = B\log_2 M\ , \qquad (15)$$

and in an *M*-QAM DMT system it is a simple sum of rates over all subcarriers

$$R = \sum_{i=1}^{K} B_i \log_2 M_i = B\log_2 M\ , \qquad (16)$$

where the second equality in (16) is valid when *M* is the same for all subcarriers. In (16), the influence of the cyclic prefix is not accounted for, but will be addressed later in the text. For *B=const.*, data rates can be maximized by choosing the largest order of modulation, which is limited by the *SNR*, obtained at the receiver, and the targeted BER. The analytical relations among BER, *SNR* and *M*, for OOK, PAM, BPSK and QAM can be found in e.g., [14]. Here, **Fig. 7** shows the dependence of the needed *SNR* on $R_i = \log_2 M_i$, for the mentioned MFs, when BER=10^{-6} and 10^{-3} are assumed.

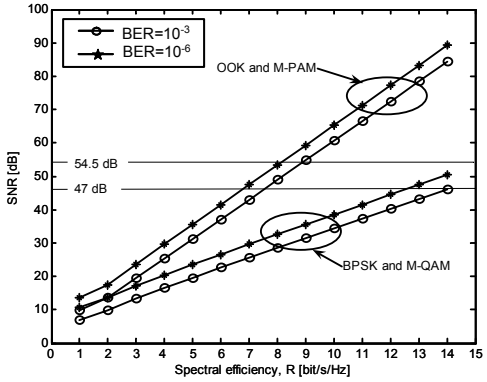


Figure 7: *SNR* requirement vs. spectral efficiency

We investigate the achievable rates for a guaranteed system performance over the "recommended surface". Starting from the *SNRs* obtained by (14) for 400 lx one can directly see from **Fig. 7** that for both BER=10^{-6} and 10^{-3}, 256-PAM can be allowed, delivering 160 Mb/s.

In the following we determine the achievable speeds with an DMT system, using *K* subcarriers. Since the subcarriers are orthogonal, signal processing after DMT demodulation can be performed at each subcarrier individually, and the *SNR*s at the different subcarriers can be considered as independent. Assuming that the total optical signal power was divided uniformly over the subcarriers (in the flat channel, the received optical power on each subcarrier will be P_R/K), the *SNR* obtained on one subcarrier can be expressed as

$$SNR_i = \left(\gamma P_{R,i}\right)^2 \Big/ \left(N_0 B_i\right) = SNR_{BB}/K\ , \qquad (17)$$

where SNR_{BB} is the *SNR* obtained for base-band transmission with (12). Hence, the SNR_i will decrease with respect to the SNR_{BB} as *K* grows and the order of the supported QAM is lower.

When discussing the potential number of sub-carriers, another aspect also needs to be addressed. DMT achieves robustness against ISI by insertion of a special guard interval called the cyclic prefix (CP), [13]. Its necessary length is determined by the channel memory. The guard band, however, introduces redundancy in the system, whose spectral efficiency then degrades to

$$\rho = R/B = K \log_2 M/(K+C), \qquad (18)$$

where C is the length of the CP expressed through the number of samples.

As already mentioned, in our system, relevant ISI could occur only between different optical LOS paths, and only if the delay is about 25 ns or more (limited symbol rate). With 25 ns also being the Nyquist sampling interval, it would be enough to dedicate to the guard interval 1-2 samples per DMT symbol. Now, for a meaningful spectral efficiency (e.g., 80%), $K \geq 4C$ is needed, rendering a choice of 8 or 16 for K.

Even though it may be argued that having DMT is unnecessary, or even not beneficial, one should aim towards a flexible system, which would be robust also in ISI-degraded environments. ISI degrades the channel response on certain frequencies. In the case of base-band transmission, performance in the whole channel is corrupted, and the *SNR* drops to 10-20 dB range (40 Mb/s with 4-PAM). DMT then allows for much better performance. In the case that the degradation involves only some sporadic frequencies, only some of the subcarriers would suffer performance degradation, whereas the rest of them would still have high *SNR*s (in the range of 50 dB). If the response is degraded on a whole frequency band, then one could deploy adaptive DMT, modulating the subcarriers with different modulation orders, depending on the *SNR* of each, as considered in [15].

In the following example we show that DMT will have an advantage over base-band transmission, even in the flat channel considered in this study. If we chose K=16 and C=2, then the obtained *SNR* on each subcarrier is 42.5 dB according to (17). From **Fig. 7**, we see that in this case 2^{11}-QAM and 2^{13}-QAM could be supported with BER=10^{-6} and 10^{-3}, respectively, which in turn render transmission speeds of 196 Mb/s and 231 Mb/s, (18).

DMT clearly outperforms base-band transmission (which offered 160 Mb/s) also in an environment without ISI, due to the advantage in power-efficiency of QAM over PAM.

4. Summary

Using white LED light simultaneously for illumination and data transmission is a promising synergy, which is increasingly gaining attention in R&D. We showed that the modulation bandwidth of commercially available LEDs can be enhanced to ~20 MHz by suppressing the phosphorescent portion of the optical spectrum. Starting from the standardized requirements for office illumination, we investigated achievable transmission rates in a medium-sized room model. We found that the transmission channel is flat, due to distributed high power via many LOS. System performances were compared, assuming base-band and DMT modulation. It was found that the deployment of DMT brings advantages even in the flat channel (due to advantage in efficiency of QAM over PAM). It can be expected that its benefits are even more pronounced in the ISI degraded environment. Achievable speeds with DMT in the investigated flat channel were about 200 Mb/s. Even though an DMT system is more complex, it can be fully realized with standard FPGAs and DSP units. Another issue for further research is the influence of transmission-line non-linearity.

5. References

[1] Y. Tanaka, *et al.*, "Indoor Visible Communication utilizing Plural White LEDs as Lighting", PIMRC 2001

[2] T. Komine *et al.*, "Fundamental Analysis for Visible-Light Communication System using LED Lightings", IEEE Trans. on Consumer Electronics, 2004

[3] P. Amirshahi and M. Kavehrad, "Broadband Access over Medium and Low Voltage Power-lines and use of White Light Emitting Diodes for Indoor Communications", IEEE CCNC, 2006

[4] T. Komine, *et al.*, „Performance Evaluation of Narrowband OFDM on Integrated System of Power Line Communication and Visible Light Communication" IEEE Symp. on Wireless Pervasive Computing, 2006

[5] M. Z. Afgani, *et al.*, "Visible Light Communication Using OFDM", IEEE TRENTCOM 2006

[6] G Pang, *et. al.*, "LED Wireless" IEEE Industry Applications Magazine, 2002

[7] www.osram.de (DOT-it)

[8] E.F.Schubert, "Light-Emitting Diodes," Cambridge University Press, 2003

[9] http://www.on-light.de/din5035.htm

[10] www.hebeiltd.com.cn (model S12NW6C)

[11] V. Jungnickel *et al.,*"A Physical Model for the Wireless Infrared Communication Channel" IEEE JSAC, 2002

[12] http://sales.hamamatsu.com

[13] D. Daly, "Efficient Multicarrier Communication on Digital Subscriber Loop," PhD thesis, University College Dublin, 2003

[14] F. Xiong, "Digital Modulation Techniques", Artech House 2000

[15] J. Grubor *et al*.,"Adaptive-Modulation Technique in Wireless Infrared Indoor Communication", ITG Fachbericht 193, pp. 193-200, 2006